Journal of Enzyme Inhibition and Medicinal Chemistry

ISSN: 1475-6366 (Print) 1475-6374 (Online) Journal homepage: http://www.tandfonline.com/loi/ienz20

Synthesis, antitumor activity evaluation of some new N-aroyl-α,β-unsaturated piperidones with fluorescence

Jufeng Sun, Suwen Wang, Hongjuan Li, Wenguo Jiang, Guige Hou, Feng Zhao & Wei Cong

To cite this article: Jufeng Sun, Suwen Wang, Hongjuan Li, Wenguo Jiang, Guige Hou, Feng Zhao & Wei Cong (2015): Synthesis, antitumor activity evaluation of some new N-aroyl-α,β-unsaturated piperidones with fluorescence, Journal of Enzyme Inhibition and Medicinal Chemistry, DOI: 10.3109/14756366.2015.1043296

To link to this article: http://dx.doi.org/10.3109/14756366.2015.1043296

Journal of Enzyme Inhibition and Medicinal Chemistry

http://informahealthcare.com/enz
ISSN: 1475-6366 (print), 1475-6374 (electronic)

J Enzyme Inhib Med Chem, Early Online: 1–8
 DOI: 10.3109/14756366.2015.1043296

Taylor & Francis
Taylor & Francis Group

Synthesis, antitumor activity evaluation of some new *N*-aroyl-α,β-unsaturated piperidones with fluorescence

Jufeng Sun[1]*, Suwen Wang[2]*, Hongjuan Li[1], Wenguo Jiang[1], Guige Hou[1], Feng Zhao[1], and Wei Cong[1]

[1]*School of Pharmacy, Binzhou Medical University, Yantai, Shandong, P.R. China and* [2]*Yantai Yuhuangding Hospital Emergency, Yantai, Shandong, P.R. China*

Abstract

Novel *N*-aroyl-α,β-unsaturated piperidones, series **1**, series **2** and series **3** (featuring 2-bromo-4,5-dimethoxybenzylidene, 4-dimethylaminobenzylidene and 4-trifluoromethylbenzylidene, respectively), were synthesized as candidate cytotoxins. Most of the compounds displayed potent cytotoxicity against the human neoplastic cell lines SK-BR-3, PG-BE1, NCI-H460, MIA PaCa-2 and SW1990 *in vitro*, and approximately 64% of the IC_{50} values were lower than 5 μM. Among those tested, compound **1b** of series **1, 3a, 3d** and **3e** of series **3** proved to be the most active. Importantly, **1b** displayed marked inhibitory effects on tumor growth *in vivo* and had no apparent toxicity to mice; this was evaluated by a nude mouse PG-BE1 xenograft model. In addition, the fluorescent properties of compounds series **1**–**3** were investigated. The interesting fluorescence exhibited by these compounds could be useful for their visualization in tumor cells, permitting further studies on these α,β-unsaturated piperidones as candidates for novel fluorescent antitumor agents.

Keywords

Antitumor agents, cytotoxicity, fluorescence, α,β-unsaturated piperidones, xenograft model

History

Received 12 January 2015
Revised 3 April 2015
Accepted 11 April 2015
Published online 15 September 2015

Introduction

Piperidone derivatives are frequently encountered in natural products and drug candidates because of their interesting biological activities and are therefore important synthetic targets[1]. Many piperidone derivatives are used widely in the synthesis of new drugs and fine chemicals because of both their pharmaceutical importance and the presence of a keto functionality with its adjacent active methylene center that can easily accommodate the introduction of other substituted groups[2]. To date, some piperidone derivatives[3–7] have been shown to possess antitumor, antidepression, antimycobacterium, antithrombotic, sedation, cholesterol-lowering and proteasome-inhibiting activities. In particular, some α,β-unsaturated piperidones, 3,5-bis(arylidene)-4-piperidones, have been reported to display cytotoxic activities[8]. Therefore, a number of novel *N*-aroyl-3,5-bis(benzylidene)-4-piperidones were designed and evaluated for their cytotoxic and antitumor activities (Figure 1). These compounds feature 2-bromo-4,5-dimethoxy, 4-dimethylamino or 4-trifluoromethyl functionality in the phenyl ring appendages, as well as various substituents at the piperidone nitrogen.

An additional consideration inspired the synthesis and evaluation of antitumor effects for these 4-piperidones. Molecules carrying one or more α,β-unsaturated keto groups show a greater preference, or sometimes an exclusive affinity, for bio-thiols over both amino and hydroxy groups. As thiols are not found in nucleic acids, these benzylidene piperidones may avoid the genotoxic effects associated with a number of currently available anticancer drugs[9–11]. Moreover, one or more thiol groups are found in a multitude of cellular constituents, for example, glutathione, cysteine and thioredoxin. Thus, thiol alkylators have the potential to covalently bond with multiple biological targets. The pharmacophore, a 1,5-diaryl-3-oxo-1,4-pentadienyl group with alicyclic unsaturated enones and cyclic piperidone, can react at each primary binding site A (Figure 2) and may allow successive chemical attacks by cellular thiols. The electron-withdrawing or electron-donating properties of different groups in the benzene rings could influence the binding effect[12,13]. In addition, the nature of the N-substituents at binding site B could affect the cytotoxic properties of the molecules. The effect could increase cytotoxic activity by facilitating the approach of the piperidone to a specific binding site or reduce the cytotoxic activity by hindering this interaction. Malignant cells are more susceptible than normal cells to this type of sequential chemical attack, so these antitumor drugs possess preferential toxicity for malignant cells over normal tissues[14]. Thus, this kind of compounds may have lower toxic side effect which is the main drawback of the current antitumor drugs to the normal cells. Moreover, they might activate caspase-3 to induce cell apoptosis or cause cell autophagy[15]. These reasons illustrate the importance of synthesizing and studying new 3,5-bis(benzylidene)-4-piperidone derivatives as antitumor drugs, which possess variable substitution on the aryl groups in the main binding site A and a range of N-substituents in the additional binding site B.

The noteworthy fluorescent properties of these molecules are another reason to synthesize and study them. In the case of cytotoxic molecules, natural fluorescence could permit tracking of the target organelle in cells. Recent investigations showed interesting fluorescent properties of a series of 3,5-bis(arylidene)-4-piperidone derivatives; some of these could be potential two-photon sensitizers because of the donor-π-acceptor-π-donor

*Jufeng Sun and Suwen Wang contributed equally to this article.

Address for correspondence: Jufeng Sun, School of Pharmacy, Binzhou Medical University, Yantai, Shandong 264003, P.R. China. Tel: +86 5356913406. Fax: +86 5356913719. E-mail: sjf.xzy@163.com

Figure 1. The structures of 3,5-bis(benzylidene)-4-piperidones synthesized are shown.

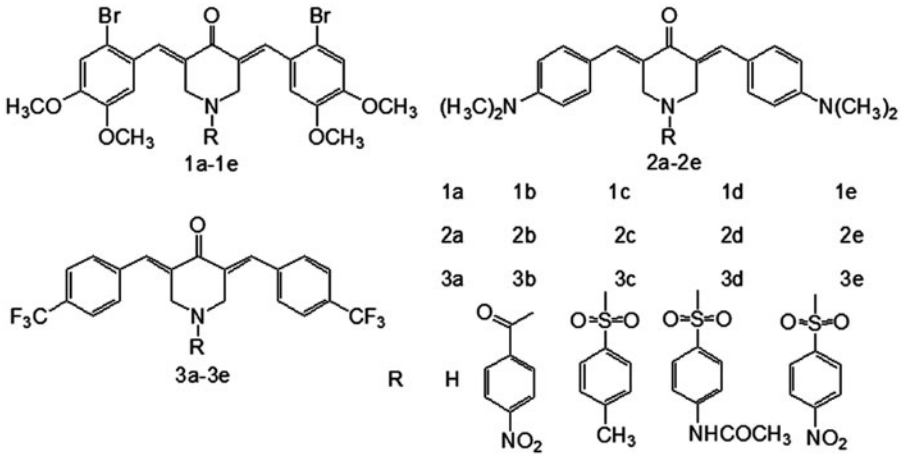

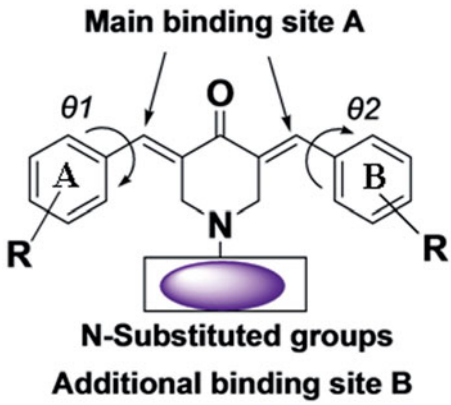

Figure 2. Binding sites A and B and designation of the torsion angles θ_1 and θ_2 of the compounds synthesized.

structure of the molecules, and their fluorescent properties may be affected by the substituents in the benzene ring[16–19]. As these types of compounds demonstrate both marked antitumor activities and fluorescent properties, they have been recognized as promising antineoplastic drug candidates.

As substituted groups in the benzene ring might affect both the cytotoxicity and fluorescent properties of these compounds, 2-bromo-4,5-dimethoxy (having both electron-withdrawing and electron-donating properties), 4-dimethylamino (electron-donating) and 4-trifluoromethyl (electron-withdrawing) functionality was introduced into these derivatives. In this study, 15 new *N*-aroyl-3,5-bis(benzylidene)-4-piperidones are reported. Their cytotoxic and antitumor activities were evaluated by a CCK-8 method and xenograft model, and their fluorescent properties were investigated.

Experimental

Materials and methods

Samples for ultraviolet (UV) studies were prepared as 10^{-4} M in a mixture of ethanol and dimethyl sulfoxide (V_{ethanol}–$V_{\text{dimethyl sulfoxide}} = 4{:}1$), and spectra were obtained with a Beckman Du-70 ultraviolet spectrophotometer (Beckman, Reja, FL). Elemental analyses were performed on a Perkin-Elmer Model 240c analyzer (Perkin-Elmer, Wellesley, MA). ^{1}H NMR data of **1a**, **1e**, **2a** and **3a** were collected using a Bruker Avance-500 MHz spectrometer (Bruker, Billerica, MA), and others were collected using a Bruker Avance-400 MHz spectrometer (Bruker, Billerica, MA). All ^{13}C NMR data were collected at 150 MHz using a Bruker Avance-600 MHz spectrometer (Bruker, Billerica, MA). Chemical shifts are reported in δ relative to TMS. All fluorescence measurements were carried out on a Cary Eclipse Spectrofluorimeter (Varian, Australia) equipped with a xenon lamp and quartz carrier at room temperature. Biological evaluation was performed using a Microplate Reader 450 (Bio-Rad, Hercules, CA) enzyme-labeled instrument.

Synthesis of 1a, 2a, 3a

4-Piperidone hydrochloride monohydrate **2** (0.01 mol) and the appropriate aryl aldehyde (0.02 mol) were mixed into glacial acetic acid (50 mL). The mixture was piped into dry hydrogen chloride gas for 0.5 h, until a clear solution was obtained. After stirred for about 24 h at room temperature, the precipitate was collected and washed with 40% sodium hydroxide in water. The free base was collected and washed with water until pH 7, then dried under the vacuum at 50–65 °C for 2 h. The compounds were recrystallized from methanol (**1a**); methanol–ethanol–chloroform (**2a**) and methanol–chloroform (**3a**). The melting points (°C) and yields (%) of **1a**–**3a** were as follows: **1a**: 246–247, 48%; **2a**: 270–272, 72%; **3a**: 227–228, 59%. ^{1}H NMR, ^{13}C NMR and elemental analysis data for compounds **1a**, **2a**, and **3a** are available in supplementary material.

Synthesis of 1b, 2b, 3b

Two milliliters of a 25% (w/v) aqueous sodium hydroxide solution containing a catalytic amount of tetrabutylammonium bromide and a suspension of **1a**, **2a** or **3a** (1 mmol) in 1,2-dichloroethane (5 mL) were combined and stirred for 15 min at 0–5 °C. 4-Nitrobenzoyl chloride (1.5 mmol) in 1,2-dichloroethane (5 mL) was then added to the flask. The resulting mixture was stirred for approximately 6–24 h at room temperature and detected by TLC (dichloromethane–methanol = 25:1). The solvent was removed under vacuum. Then, 10% potassium carbonate was added to the residue, and this was stirred for 2 h. The precipitate was collected and dried *in vacuo*. The compounds were recrystallized from methanol (**1b**), dimethylformamide (**2b**), or methanol–chloroform (**3b**). The melting points (°C) and yields (%) of **1b**–**2b** were as follows: **1b**: 236–238, 40%; **2b**: 256–259, 73%; **3b**: 209–212, 78%. ^{1}H NMR, ^{13}C NMR and elemental analysis data for compounds **1b**, **2b**, and **3b** are available in supplementary material.

General synthesis of 1c–1e, 2c–2e, 3c–3e

Two milliliters of a 25% (w/v) aqueous sodium hydroxide solution was mixed with a suspension of **1a**, **2a** or **3a** (1 mmol) in

1,2-dichloroethane (5 mL). A catalytic amount of tetrabutylammonium bromide was added to the mixture, and this was stirred for 10 min at 0–5 °C. To the mixture was added alternatively 4-methylbenzenesulfonyl chloride or 4-acetaminobenzenesulfonyl chloride or 4-nitrobenzenesulfonyl chloride (1.5 mmol) in 1,2-dichloroethane (5 mL). The resulting solution was stirred for approximately 7–24 h at room temperature and detected by TLC (chloroform–methanol = 25:1). After the reaction was complete, glacial acetic acid was added to the mixture until achieving pH 3. The precipitate was collected, washed with water and dried *in vacuo*. The compounds were recrystallized from methanol or methanol–chloroform (**1c–1e**), dimethylformamide or acetone (**2c–2e**), or methanol, 95% ethanol or chloroform (**3c–3e**). The melting points (°C) and yields (%) of **1c–1e, 2c–2e, 3c–3e** were as follows: **1c**: 229–231, 68%; **1d**: 255–256, 81%; **1e**: 238–239, 49%; **2c**: 239–240, 63%; **2d**: 255–256, 47%; **2e**: 248–249, 75%; **3c**: 182–183, 79%; **3d**: 216–219, 45%; **3e**: 235–236, 74%. ^{1}H NMR, ^{13}C NMR and elemental analysis data for compounds **1c–1e**, **2c–2e**, and **3c–3e** are available in supplementary material.

A chloroform solution of **1e** (7.4 mg, 0.01 mmol) was kept at room temperature. Upon slow evaporation of the solvent about 15 days, bright yellow crystals of **1e** were obtained.

Biological evaluation

Cell cytotoxicity assay by cell counting kit-8

Compounds belonging to series **1–3** were screened against five tumor cell lines (Peking union medical college), namely SW1990 and MIA PaCa-2 (human pancreatic carcinoma), PG-BE1 and NCI-H460 (human lung carcinoma) and SK-BR-3 (human breast cancer) using a cell counting kit-8 (WST-8, Dojindo Laboratories, Tokyo, Japan) method. Cells were cultured in RPMI-1640 medium (Sigma-Aldrich, St. Louis, MO) supplemented with 10% fetal bovine serum (FBS, HyClone, Logan, UT), 2 mM L-glutamine and 50 μg/mL gentamycin. Cytotoxicity for each individual compound was measured after 48 h of cocultivation with each cell line. Briefly, the different cell lines were seeded into 96-well plates at a concentration of 1×10^4 cells/100 μL/well. The cells were allowed to attach overnight at 37 °C in a humidified atmosphere containing 5% CO_2. The tested compounds were initially dissolved in DMSO (Sigma-Aldrich), and the working solutions were added to a FBS free culture medium. The final DMSO concentration in each well was 1%. The compounds were added to wells with increasing drug concentrations. After a 48-h incubation period, 10 μL of CCK-8 reagent was added, and the plate was incubated for 4 h at 37 °C. The optical density (OD) was measured by a multi-well plate reader (TECAN, Männedorf, Switzerland) at 450 nm. The results are expressed as a decrease in the cell viability (%) in comparison to untreated controls. The concentration of each compound was examined in triplicate, and the IC_{50} values are expressed graphically. The concentrations of the compounds used were 200, 100, 10, 1, 0.1 and 0.01 μg/mL. 5-Fluorouracil (5-FU, Sigma-Aldrich) was used as a positive control. The concentrations of 5-FU used were 250, 25, 2.5, 0.25 and 0.025 μg/mL.

Tumor xenograft model

The human lung carcinoma PG-BE1 xenograft model was set up. The BALB/c female athymic nude mice (BALB/c, nu/nu) were purchased from the Institute for Experimental Animals, Chinese Academy of Medical Sciences & Peking Union Medical College. The study protocols were according to the regulations of Good Laboratory Practice for non-clinical laboratory studies of drugs issued by the National Scientific and Technologic Committee of People's Republic of China. The treatment and use of animals during the study was permitted by the Animal Ethics Committee of the Institute of Medicinal Biotechnology, Chinese Academy of Medical Sciences & Peking Union Medical College (permission number: c1-2011-1121).

PG-BE1 cells growing in exponential phase were implanted into the 6–8-week-old female athymic nude mice by subcutaneous injection of 10×10^6 cells on the right flank. After 3 weeks, the tumors were dissected aseptically, and pieces of tumor tissue (2 mm^3 in size) were transplanted into athymic mice subcutaneously. When the size of tumors reached approximately 100 mm^3, the mice were divided into groups at random ($n = 6$ per group) and treated with 5-FU, compound **1b** at different doses twice weekly for 3 weeks, respectively. Control group was injected with saline. The tumor diameter was measured with a caliper, and tumor volumes were calculated with the following formula: $V = 0.5a \times b^2$, where a and b are the long and the perpendicular short diameters of the tumor, respectively. Typically, the experiments were concluded when tumors in the control animals were close to an average size of 2000 mm^3. The tumor inhibitory rate was calculated as IR% = {1 − [(tumor volume$_{final}$ − tumor volume$_{initial}$ for the treated group)/(tumor volume$_{final}$ − tumor volume$_{initial}$ for the control group)]} × 100%.

Single-crystal structure determination

X-Ray intensity data were measured at 298(2) K on a Bruker SMART APEX CCD-based diffractometer (Mo Kα radiation, $\lambda = 0.71073$ Å) using a SMART and SAINT programs (Bruker, Billerica, MA). The structures were solved by direct methods and refined on F^2 by full-matrix least-squares methods with SHELXTL version 6.1 (Göttingen, Germany). Crystal data of **1e**: $C_{31}H_{28}Br_2Cl_6N_2O_9S$, $M = 977.13$, triclinic, space group P-1, yellow block, $a = 10.322(9)$), $b = 11.353(10)$ Å, $c = 18.561(16)$ Å, $\alpha = 87.462(13)°$, $\beta = 86.197(11)°$, $\gamma = 68.646(10)°$, $V = 2021(3)$ Å^3, $Z = 2$, $D_c = 1.606$ g cm^{-3}, μ(Mo Kα) = 2.505 mm^{-1}, $T = 298(2)$ K; 7168 unique reflections [$R_{int} = 0.0282$]. Final R_1 [with $I > 2\sigma(I)$] = 0.0580, wR_2 (all data) = 0.1457.

CCDC 918752 (**1e**) contains the supplementary crystallographic data for this article. Copies of the data can be obtained free of charge on application to CCDC, 12 Union Road, Cambridge CB2 1EZ, UK (Fax: + 44 1223336033; e-mail: deposit@ccdc.cam.ac.uk).

Results and discussion

Synthesis and structures

Fifteen new compounds **1a–1e** (series **1**), **2a–2e** (series **2**) and **3a–3e** (series **3**) were prepared by the synthetic route shown in Scheme 1. Dry hydrogen chloride was used to catalyze the reaction of various aryl aldehydes with 4-piperidone via a Claisen–Schmidt condensation, leading to the preparation of **1a**, **2a** and **3a**. Treatment of these compounds with each of 4-nitrobenzoyl chloride, 4-methylbenzenesulfonyl chloride, 4-acetamidobenzenesulfonyl chloride or 4-nitrobenzenesulfonyl chloride produced the corresponding *N*-acylated or *N*-sulfonylated derivatives **1b–1e, 2b–2e** and **3b–3e**. The yields of the compounds were between 40% and 81%. Their structures were fully characterized by ^{1}H NMR, ^{13}C NMR and elemental analysis. ^{1}H NMR spectroscopy indicated that molecules in series **1–3** were stereoisomerically pure. The NMR signals of CH_2 groups in the central piperidone ring were split due to the influence of noncoplanarity between two aryl rings of the parent NH-3,5-bis(benzylidene)-4-piperidones and the adjacent olefinic linkages for some compounds, most notably for **1b, 2b, 3b** and **3e**. Some carbon signals in the ^{13}C NMR spectra for the two aryl rings (attached to the olefinic bonds) were similarly influenced

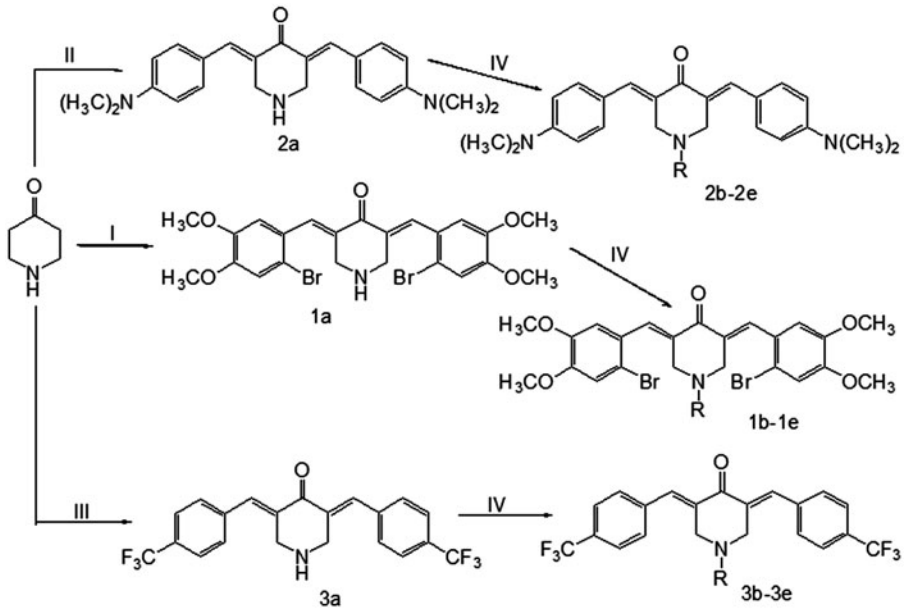

Scheme 1 Synthetic chemical pathway of compounds in series **1**–**3**. The reagents used in the syntheses were as follows: (I) 2-bromo-4,5-dimethoxy-benzaldehyde/CH_3COOH/dry HCl; (II) 4-dimethylamino-benzaldehyde/CH_3COOH/dry HCl; (III) 4-trifluoromethyl-benzaldehyde/CH_3COOH/dry HCl; (IV) 4-nitrobenzoyl chloride/NaOH/$ClCH_2CH_2Cl$/K_2CO_3/tetrabutylammonium bromide or 4-methylbenzene sulfonyl chloride/ 4-acetamidobenzenesulfonyl chloride/ 4-nitrobenzenesulfonyl/NaOH/$ClCH_2CH_2Cl$/ tetrabutylammonium bromide/CH_3COOH.

Table 1. Cytotoxicity of **1a**–**1e, 2a**–**2e** and **3a**–**3e** against human SK-BR-3, PG-BE1, NCI-H460, MIA PaCa-2 and SW1990 cell lines.

	IC_{50} (μM)				
Compound	SK-BR-3	PG-BE1	NCI-H460	MIA PaCa-2	SW1990
1a	4.38 ± 0.48	1.31 ± 0.04	0.960 ± 0.108	0.377 ± 0.027	1.91 ± 0.37
1b	3.19 ± 0.53	0.382 ± 0.098	0.402 ± 0.056	0.167 ± 0.017	0.978 ± 0.496
1c	10.8 ± 1.9	3.16 ± 0.73	3.44 ± 0.67	1.24 ± 0.35	3.66 ± 0.28
1d	2.86 ± 0.35	1.77 ± 0.28	1.39 ± 0.51	0.29 ± 0.06	1.72 ± 0.37
1e	23.1 ± 1.1	2.27 ± 0.54	1.41 ± 0.30	1.33 ± 0.07	4.74 ± 0.76
2a	64.0 ± 10.5	11.3 ± 2.77	11.8 ± 3.6	8.23 ± 0.33	36.7 ± 5.0
2b	>100	>100	>100	>100	>100
2c	13.6 ± 1.5	23.4 ± 2.4	9.66 ± 3.79	8.82 ± 1.48	12.6 ± 3.4
2d	>100	>100	>100	>100	>100
2e	>100	>100	>100	>100	>100
3a	0.843 ± 0.092	0.661 ± 0.046	1.04 ± 0.21	0.417 ± 0.094	1.94 ± 0.24
3b	3.70 ± 0.14	4.08 ± 0.32	3.38 ± 0.11	0.230 ± 0.016	1.51 ± 0.48
3c	4.40 ± 0.15	1.75 ± 0.44	0.544 ± 0.243	0.593 ± 0.132	3.69 ± 0.21
3d	1.12 ± 0.24	0.820 ± 0.085	0.321 ± 0.081	0.353 ± 0.016	0.755 ± 0.553
3e	0.417 ± 0.080	0.565 ± 0.042	0.126 ± 0.031	0.107 ± 0.006	0.365 ± 0.109
5-FU	1297 ± 330	94.3 ± 23.9	35.8 ± 11.6	102 ± 9	474 ± 96

and split, for example in compound **2b**[8,13,20–22]. An X-ray crystallographic structure of **1e** showed that it adopted an *E,E* configuration.

The UV spectra of the molecules were inspected at a concentration of 10^{-4} mol L^{-1} in a mixture of ethanol and dimethyl sulfoxide. From the spectra, two λ_{max} values could be seen for almost all the derivatives except **3a** and **3e**. The main λ_{max} values ranged from 374 to 383 nm for series **1**, 461–472 nm for series **2** and 303–311 nm for series **3**. The λ_{max} values increased from series **2** to series **1** to series **3** due to the extension of the π-conjugation system in the molecules. This was caused mainly by the change of substituents in the benzene rings of the parent NH-3,5-bis(4-dimethylaminobenzylidene)-4-piperidone for series **2**, NH-3,5-bis(2-bromo-4,5-dimethoxybenzylidene)-4-piperidone for series **1** and NH-3,5-bis(4-trifluoromethylbenzylidene)-4-piperidone for series **3**. The electron-withdrawing effects of the substituents strengthened gradually from series **2**, to series **1**, to series **3**; thus, the π-conjugation system lengthened in the order of series **3**, series **1** and series **2**. These differing properties caused a change in the appearance of the compounds. Series **3** compounds are mainly pale yellow crystals, series **1** compounds are generally yellow or bright yellow crystals and series **2** compounds are a red or red-orange powder. The melting points for compounds in these series decrease according to the following: **2** > **1** > **3** when comparing three compounds having identical substituents attached to the piperidyl nitrogen atom. This is related to increases in electron-donating effects of aryl substituents in the parent benzene rings.

Antitumor activity

Cell cytotoxicity

The cytotoxic activities of the synthetic compounds were evaluated against five human carcinoma cell lines: SW1990, MIA PaCa-2, PG-BE1, NCI-H460 and SK-BR-3. The results are shown in Table 1, which summarizes the corresponding IC_{50} values (the IC_{50} represents the drug concentration resulting in 50% growth inhibition).

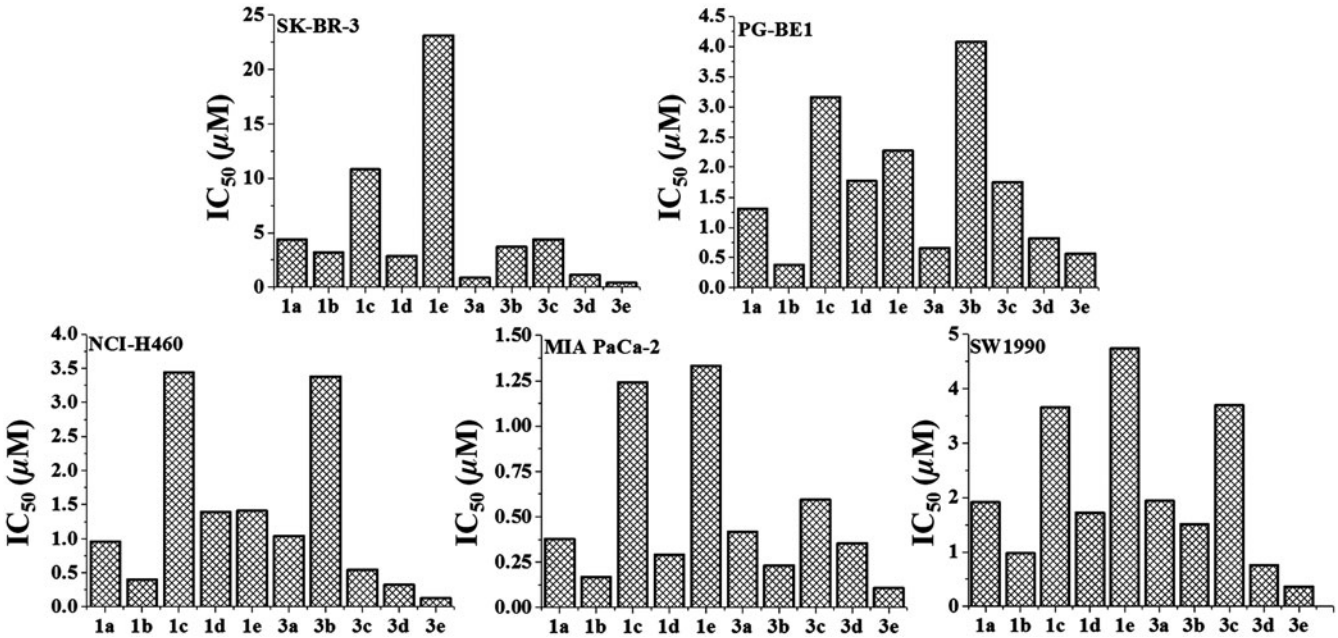

Figure 3. The inhibitory effect of compounds **1a**–**1e** and **3a**–**3e** against five human carcinoma cell lines.

Figure 4. The ORTEP figure of **1e** (displacement ellipsoids with 30% probability, omitting two molecules of $CHCl_3$).

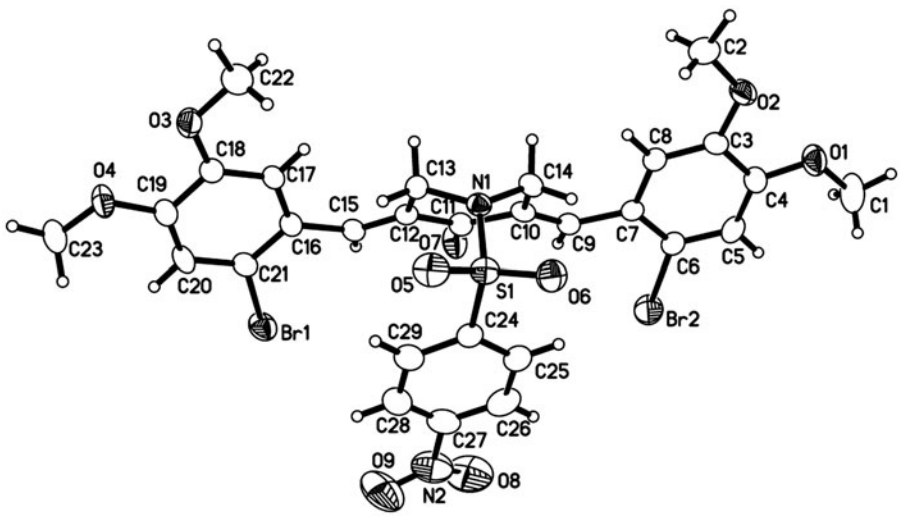

As shown in Table 1, the biological evaluation data showed that 96% of the IC_{50} values of the compounds in series **1** and **3** against SW1990, NCI-H460, PG-BE1, MIA PaCa-2 and SK-BR-3 cells were lower than 5 μM, while 44% of these values were submicromolar. These data revealed that almost all the compounds in series **1** and **3** were potent inhibitors of the growth of various malignant cells; the especially high potencies of **1b, 3a, 3d** and **3e** should be noted. In the case of series **2**, only **2a** and **2c** showed moderate potency, while the IC_{50} values of **2b, 2d** and **2e** were all greater than 100 μM. As displayed in Figure 3, among compounds **1a**–**1e** and **3a**–**3e**, the SW1990, MIA PaCa-2, NCI-H460 and SK-BR-3 cell lines were the most sensitive toward compound **3e**, while the PG-BE1 cell line was the most sensitive to compound **1b**.

To verify the discrepancy between potencies, some investigations were conducted. As mentioned previously, biological potencies may be influenced by the nature of the aryl substituents in rings A and B (Figure 2). It can be seen in Table 1 that compounds **2a**–**2e**, which have strong electron-donating dimethylamino groups in the *para*-position of the parent benzene rings, were the least active among the three series. Comparing compounds **3a**–**3e**, with only electron-withdrawing trifluoromethyl groups in the parent benzene rings, and compounds **1a**–**1e**, bearing both electron-withdrawing bromine groups and electron-donating methoxy groups in the parent benzene rings, more than 80% of the IC_{50} values for **3a**–**3e** were higher than or similar to those of the corresponding compounds of **1a**–**1e**. Compound **3b** was the only compound in series **3** that exhibited lower IC_{50} values against all five human carcinoma cell lines than compound **1b** in series **1**. In addition, the nature of N-substituted groups may also be one of the factors that can affect the cytotoxic potencies. As presented in Table 1, the potencies of *N*-aroyl analogs **1b, 1d, 3b, 3d** and **3e** against SW1990 were higher than those of the parent NH-4-piperidones **1a** and **3a**. This difference demonstrated that about half of the *N*-aroyl analogs had potencies that were intensified in series **1** and **3**. In particular, the IC_{50}

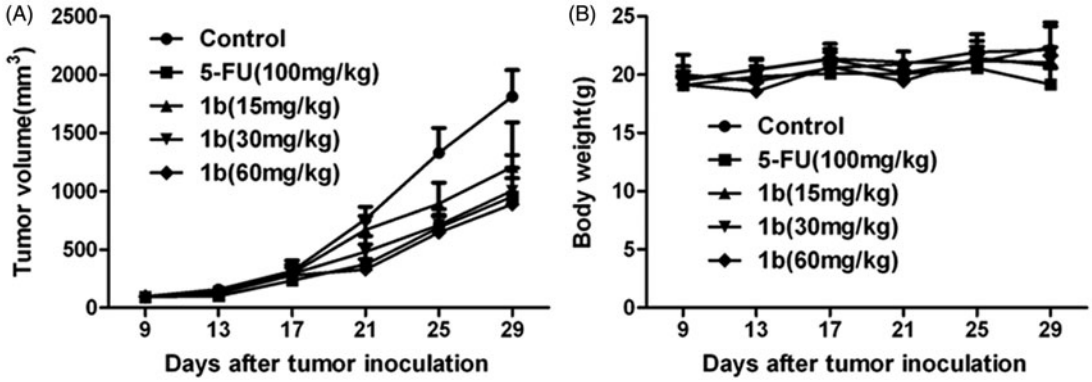

Figure 5. (A) The tumor growth inhibition of compound **1b** against nude mice with PG-BE1 xenograft (in the light of tumor volume). (B) The effect of compound **1b** on the body weight of nude mice with PG-BE1 xenograft.

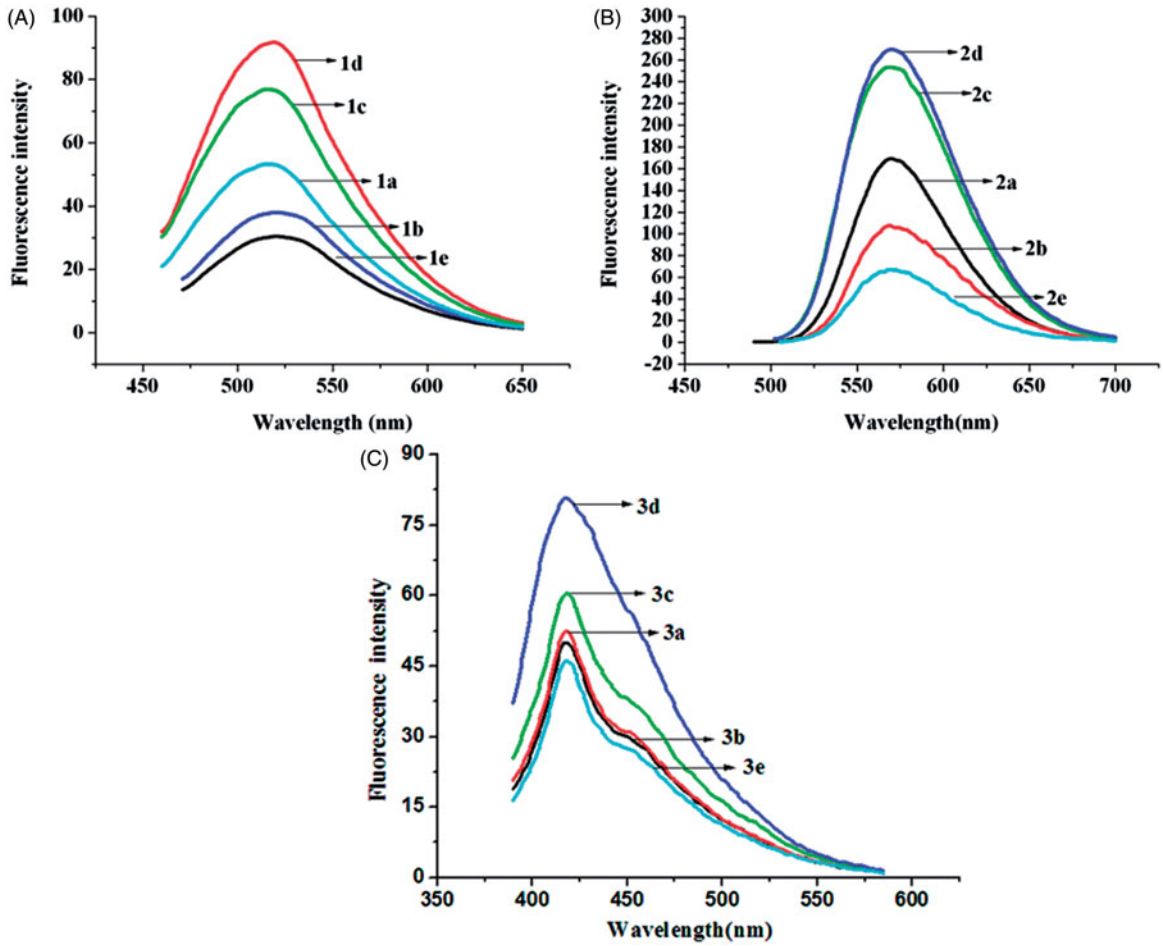

Figure 6. (A) The fluorescence spectra of **1a**–**1e** at room temperature. (B) The fluorescence spectra of **2a**–**2e** at room temperature. (C) The fluorescence spectra of **3a**–**3e** at room temperature.

values of compounds **1b** and **3e** against all five carcinoma cell lines were higher than those of **1a** and **3a** separately.

Moreover the noncoplanarity between the two aryl rings of the parent NH-3,5-bis(benzylidene)-4-piperidones and the adjacent olefinic linkages might allow a favorable topography for the alignment of these compounds with their targets at cellular binding sites (Figure 2), thereby increasing the cytotoxicity of the molecules[22]. To confirm this, the X-ray crystallographic structure of the representative compound *N*-(4-nitrobenzensulfonyl)-3,5-bis(2-bromo-4,5-dimethoxybenzylidene)-4-piperidone (**1e**) was investigated. The ORTEP diagram of **1e** is presented in Figure 4. The X-ray crystallographic structure revealed that compound **1e** crystallizes in the triclinic space group *P*-1 with two $CHCl_3$ molecules. As shown in Figure 4, a single-crystal structure of **1e** shows the *E* stereochemistry of the olefinic double bonds (*E,E* isomer), which is confirmed by the C12–C15–C16–C17 torsion angle value ($\theta_1 = 28.915(7)^\circ$) and C10–C9–C7–C8 torsion angle value ($\theta_2 = -30.15(8)^\circ$). It is noteworthy that, in

this structure, the 4-nitrophenylsulfonyl group is almost parallel to the C14–C10–C11–C12–C13 plane and the two aryl groups in 3,5-bis(benzylidene)-4-piperidones. The corresponding dihedral angles are ca. 25.9(2)°, *ca*. 6.52(2)° and ca. 9.35(2)°. In addition, the N1–S1–C24 angle is only 108.0(2)°, which demonstrates that the olefinic double bonds are close to the 4-nitrophenylsulfonyl group. The corresponding C12···C24, C15···C29, C10···C24 and C9···C25 distances are 3.372(2), 3.612(2), 3.541(3) and 3.777(3) Å. Such short distances may result in inter-conjugated-system interactions between the 4-nitrophenylsulfonyl groups and 3,5-bis(benzylidene)-4-piperidones, further influencing the fluorescent properties of the molecules.

Antitumor activity *in vivo*

The antitumor activity *in vivo* is the most important factor to evaluate for new antitumor agents. The sensitive PG-BE1 xenograft model was used to investigate the antitumor activity *in vivo* of compound **1b**, which had higher potency. The diameters of tumors were measured two times per week after treatment of **1b** in athymic nude mice with PG-BE1 xenografts (Figure 5A). With doses of 60, 30 and 15 mg/kg, the corresponding tumor inhibitory rates were 58.8%, 38.3% and 31.0%, respectively, which demonstrated that compound **1b** could inhibit the growth of the tumor. Moreover, toxicity is one of the metrics to judge antitumor agents, and the body weight changes of nude mice post-therapy can be influenced by the toxicity of the drugs indirectly. From Figure 5(B), it was shown that the body weight of mice did not decreased obviously compared with the control group, indicating that compound **1b** has no apparent toxicity to nude mice bearing PG-BE1 xenografts.

Fluorescent properties

Lengthening the conjugated spacer by inserting additional substituted groups into 3,5-bis(arylidene)-4-piperidone may result in increasing the electron-transporting effects and fluorescent properties of the molecules[23,24]. Taking this into account, the *N*-aroyl-3,5-bis(arylidene)-4-piperidone derivatives, discussed above, were designed and synthesized. Their fluorescent properties were then explored (Figure 6A–C).

The compounds were excited at 435 nm for series **1**, 365 nm for series **2** and 373 nm for series **3** to obtain the fluorescence spectra. The solutions (10^{-4} mol L^{-1}) were prepared in a mixture of ethanol and dimethyl sulfoxide ($V_{ethanol}$–$V_{dimethyl\ sulfoxide}$ = 4:1). The fluorescence emission was measured at room temperature from 460 to 650 nm for series **1**, 480–700 nm for series **2** and 390–590 nm for series **3**. Figure 6(A)–(C) displays contrasts in the emission spectra from series **1** to series **3**, respectively. Compounds of series **1** exhibit an emission maximum at approximately 521 nm, compounds of series **2** at approximately 572 nm and compounds of series **3** at approximately 424 nm.

The results of Figure 6(A)–(C) revealed that compounds **2a**–**2e**, with strong electron-donating dimethylamino groups, possessed the strongest fluorescence. The fluorescence intensities of compounds **1a**–**1e** and **3a**–**3e** were weaker due to the influence of the heavy atom effect from bromine and the electron-withdrawing effects of trifluoromethyl groups, respectively. In addition, the emission intensity of the parent NH-3,5-bis(benzylidene)-4-piperidones (**1a**, **2a**, **3a**) is stronger than that of *N*-(4-nitrobenzoyl) derivatives (**1b**, **2b**, **3b**) and *N*-(4-nitrobenzenesulfonyl) derivatives (**1e, 2e, 3e**), but weaker than that of *N*-(4-acetaminobenzenesulfonyl) derivatives (**1d, 2d, 3d**) and *N*-(4-methylbenzenesulfonyl) derivatives (**1c, 2c, 3c**).

At the same time, the results indicated that the fluorescent properties of these compounds were correlated with their cytotoxic activities. It can be seen from Table 1 and Figure 6(A)–(C) that compounds **2a**–**2e**, with stronger fluorescence intensity, demonstrated lower cytotoxic activities, while compounds **1a**–**1e** and **3a**–**3e**, with weaker fluorescent intensity, demonstrated higher cytotoxic activities. Further investigation into the structure–cytotoxicity–fluorescence relationships of the compounds is warranted.

Conclusions

In summary, we synthesized 15 new α,β-unsaturated piperidones (*N*-aroyl-3,5-bis(benzylidene)-4-piperidones), **1a**–**1e** (series **1**), **2a**–**2e** (series **2**) and **3a**–**3e** (series **3**), and investigated their cytotoxic and fluorescent properties. In addition, we assessed the antitumor activity *in vivo* of compound **1b** (having better potency) using a nude mouse PG-BE1 xenograft model. Among the derivatives assayed, the majority of compounds **1a**–**1e** (possessing strong electron-withdrawing trifluoromethyl groups in the aryl rings of A and B) and **3a**–**3e** (possessing both electron-withdrawing bromine and electron-donating methoxy groups in aryl rings A and B) displayed significant cytotoxic properties, but their fluorescent activities were a little weaker. Alternatively, molecules **2a**–**2e** (bearing strong electron-donating dimethylamino groups in the aryl rings A and B) illustrated poor cytotoxic properties, but their fluorescent activities were stronger than those of compounds **1a**–**1e** and **3a**–**3e**. Nevertheless, all the compounds that were investigated had interesting fluorescent properties overall. Compounds **1b, 3a, 3d** and **3e** displayed remarkable cytotoxic activities towards five human carcinoma cell lines. Importantly, the results of a PG-BE1 xenograft model showed that compound **1b** possessed marked inhibitory effects on tumor growth and had no obvious toxicity toward the nude mice. Compounds **1b, 3a, 3d** and **3e** represent possible lead molecules for synthesizing new derivatives with the aim to increase their cytotoxic potencies, while producing low-toxicity antitumor drug candidates that undergo fluorescence.

Declaration of interest

Financial support of this work was from National Natural Science Foundation of China (No. 21402010), the Foundation of Shandong Province (Nos. ZR2014BL008, ZR2010HL065). The authors report no declarations of interest.

References

1. Shintani R, Tokunaga N, Doi H, et al. A new entry of nucleophiles in rhodium-catalyzed asymmetric 1,4-addition reactions: addition of organozinc reagents for the synthesis of 2-aryl-4-piperidones. J Am Chem Soc 2004;126:6240–1.
2. Weintraub PM, Sabol JS, Kane JM, Borcherding DR. Recent advances in the synthesis of piperidones and piperidines. Tetrahedron 2003;59:2953–89.
3. Dimmock JR, Ealias DW, Beazely MA, et al. Bioactivities of chalcones. Curr Med Chem 1999;6:1125–49.
4. Feenstra RW, Long SK, vander Heijden JAM, et al. Use of compounds having combined dopamine D-$5HT_{1A}$ and α-adrenoreceptor agonist action for treating central nervous system disorders. US Patent 2003/0186838 A1; 2003.
5. Comins DL, Brooks CA, Ingalls CL. Reduction of *N*-acyl-2-3-dihydro-4-pyridones to *N*-acyl-4-piperidones using zinc and acetic acid. J Org Chem 2001;66:2181–2.
6. Baldwin PR, Reeves AZ, Powell KR, et al. Monocarbonyl analogs of curcumin inhibit growth of antibiotic sensitive and resistant strains of mycobacterium tuberculosis. Eur J Med Chem 2015;92:693–9.
7. Bazzaro M, Anchoori RK, Mudiam MKR, et al. α,β-Unsaturated carbonyl system of chalcone-based derivatives is responsible for broad inhibition of proteasomal activity and preferential killing of human papilloma virus (HPV) positive cervical cancer cells. J Med Chem 2011;54:449–56.

8. Duffield KM, Jha A. 3,5-Bis(arylmethylene)-4-piperidone derivatives as novel anticancer agents. Indian J Chem 2006;45B: 2313–20.
9. Chen G, Waxman DJ. Role of cellular glutathione and glutathione *S*-transferase in the expression of alkylating agent cytotoxicity in human breast cancer cells. Biochem Pharmacol 1994;47:1079–87.
10. Tsutsui K, Komuro C, Ono K, et al. Chemosensitization by buthionine sulfoximine *in vivo*. Int J Radiat Oncol Biol Phys 1986;12:1183–6.
11. Das S, Das U, Sakagami H, et al. Dimeric 3,5-bis(benzylidene)-4-piperidones: a novel cluster of tumour-selective cytotoxins possessing multidrug-resistant properties. Eur J Med Chem 2012;51: 193–9.
12. Das U, Sharma RK, Dimmock JR. 1,5-Diaryl-3-oxo-1,4-pentadienes: a case for antineoplastics with multiple targets. Curr Med Chem 2009;16:2001–20.
13. Das S, Das U, Sakagami H, et al. Sequential cytotoxicity: a theory examined using a series of 3,5-bis(benzylidene)-1-diethylphosphono-4-oxopiperidines and related phosphonic acids. Bioorg Med Chem Lett 2010;20:6464–8.
14. Pati HN, Das U, Quail JW, et al. Cytotoxic 3,5-bis(benzylidene)-piperidin-4-ones and *N*-acyl analogs displaying selective toxicity for malignant cells. Eur J Med Chem 2008;43:1–7.
15. Das U, Sakagami H, Chu Q, et al. 3,5-Bis(benzylidene)-1-[4-2-(morpholin-4-yl)ethoxyPhenylcarb-onyl]-4-piperidone hydrochloride: a lead tumor-specific cytotoxin which induces apoptosis and autophagy. Bioorg Med Chem Lett 2010;20:912–17.
16. Nesterov VN, Timofeeva TV, Sarkisov SS, et al. 3,5-Bis[4-(diethylamino)benzylidene]-1-methyl-4-piperidone and 3,5-bis-[4-(diethyl amino)cinnamylidene]-1-methyl-4-piperidone: prospective biophotonic materials. Acta Cryst 2003;C59:o605–8.
17. Short KW, Kinnibrugh TL, Sammeth DM, et al. Spectroscopic, cyto-, and photo-toxicity studies of substituted piperidones: potential sensitizers for two-photon photodynamic therapy. Proc SPIE 2009;7164:716411–19.
18. Makarov MV, Leonova ES, Rybalkina EY, et al. Methylenebisphosphonates with dienone pharmacophore: synthesis, structure, antitumor and fluorescent properties. Arch Pharm Chem Life Sci 2012;345:349–59.
19. Nesterov VN. 3,5-Bis(4-methoxybenzylidene)-1-methyl-4-piperidone and 3,5-bis(4-methoxybenzylidene)-1-methyl-4-oxopiperidiniumchloride: potential biophotonic materials. Acta Cryst 2004; C60:o806–9.
20. Jha A, Mukherjee C, Prasad AK, et al. *E,E,E*-1-(4-Arylamino-4-oxo-2-butenoyl)-3,5-bis(arylidene)-4-piperidones: a topographical study of some novel potent cytotoxins. Bioorg Med Chem 2007;15: 5854–65.
21. Das S, Das U, Selvakumar P, et al. 3,5-Bis(benzyli dene)-4-oxo-1-phosphonopiperidines and related diethyl esters: potent cytotoxins with multi-drug-resistance reverting properties. ChemMedChem 2009;4:1831–40.
22. Das U, Alcorn J, Shrivastav A, et al. Design, synthesis and cytotoxic properties of novel 1-[4-(2-alkylaminoethoxy) phenylarbonyl]-3,5-bis(arylidene)-4-piperidones and related compounds. Eur J Med Chem 2007;42:71–80.
23. Hou GG, Ma JP, Wang L, et al. Co-crystallization of oxadiazole-bridged pyridyl-*N*-oxide building modules with R-aromatics (R = –OH, $–NH_2$ and –COOH). CrystEngComm 2010;12:4287–303.
24. Hou GG, Zhao HJ, Sun JF, et al. Synthesis, structure and luminescence of co-crystals with hexagonal channels: arranging disposition and π–π interactions. CrystEngComm 2013;15:577–85.

Supplementary material available online
Supplementary information